Site-Specific Vanadates $Co_4Fe_{3.33}(VO_4)_6$ and $Mn_3Fe_4(VO_4)_6$

Xiandong Wang, Douglas A. Vander Griend, Charlotte L. Stern, and Kenneth R. Poeppelmeier*

Department of Chemistry, Northwestern University, Evanston, Illinois 60208-3113

Received August 3, 1999

Single crystals of $Co_4Fe_{3.33}(VO_4)_6$ and $Mn_3Fe_4(VO_4)_6$ were grown from equivalent $CoO/Fe_2O_3/V_2O_5$ and $MnO/Fe_2O_3/V_2O_5$ melts, respectively. The former crystallizes in the orthorhombic space group *Pnma* with parameters $a = 4.965(1)$ Å, $b = 10.211(1)$ Å, $c = 17.188(3)$ Å, and $Z = 2$ and is a homeotype of such catalysts as $Mg_{2.5}VMoO_8$. The latter crystallizes in the triclinic space group $P\bar{1}$ with parameters $a = 6.703(2)$ Å, $b = 8.137(1)$ Å, $c = 9.801(2)$ Å, $\alpha = 105.56(1)°$, $\beta = 105.58(2)°$, $\gamma = 102.35(1)°$, and $Z = 1$ and is a homeotype of β-$Cu_3Fe_4(VO_4)_6$, the low-pressure form of α-$Cu_3Fe_4(VO_4)_6$. The cobalt analogue deviates in stoichiometry from the reactant melt to form the more dense α-$Cu_3Fe_4(VO_4)_6$ structure type comprised of partially occupied face-sharing octahedral and trigonal prismatic coordination sites.

Introduction

Multicomponent vanadates and molybdates can selectively oxidize hydrocarbons. For example, $(VO)_2P_2O_7$ and $SbVO_4$ are excellent catalysts for the oxidation of *n*-butane to maleic anhydride and ammoxidation of propene to acrylonitrile, respectively. Our present aim is to gain a better understanding of the chemistry of this type of heterogeneous catalysis by developing new vanadates/molybdates. Single-crystal growth provides an effective way to discover and characterize new compounds because it renders thermodynamically favorable compositions and facilitates precise structural determination. Since the stoichiometry of the crystal is not restricted to that of the reactants, it can vary to facilitate the formation of particular structures, and the contributions to the stability of such structures can be elucidated by comparing the flux composition to that of the resulting crystals. Finally, characterization by X-ray analysis goes beyond basic structure to explicate critical details such as composition, defect chemistry, and atomic disorder.

Previous studies on the $MO-V_2O_5-MoO_3$ (M = Mg, Zn, Mn) systems revealed that $M_{2.5}VMoO_8$ (M = Mg, Zn, and Mn)[1−4] adopt structures similar to those of such oxides as $NaCo_{2.31}(MoO_4)_3$,[5] $Cu_{3.85}(MoO_4)_3$,[6] $(Cu,Zn)_{3.75}(MoO_4)_3$,[7] and α-$Cu_3Fe_4(VO_4)_6$. The latter is the mineral lyonsite.[8] All these compounds are particularly dense ternary oxides with partially occupied face-sharing octahedral cation sites. α-$Cu_3Fe_4(VO_4)_6$ is the only vanadate with such a structure, and when prepared in the laboratory, it possesses a different structure (β-$Cu_3Fe_4(VO_4)_6$) which is considerably less dense.[9] Given that $Mg_{2.5}VMoO_8$ is a good catalyst for the oxidative dehydrogenation of butane to butene and butadiene,[10] we have attempted to synthesize similar vanandates by substituting into $Cu_3Fe_4(VO_4)_6$. Attempts to replace CuO led us to investigate the $MO-Fe_2O_3-V_2O_5$ (M = Mg, Zn, Co, Mn) systems since these divalent metals occur in the aforementioned vanadomolybdates. In the first two systems, the ternary vanadates $FeMg_2V_3O_{11}$ and $FeZn_2V_3O_{11}$ were found with the $GaZn_2V_3O_{11}$ structure type.[11] In the last two systems, the new ternary vanadates $Co_4Fe_{3.33}(VO_4)_6$ and $Mn_3Fe_4(VO_4)_6$ were found to be homeotypes of the α-$Cu_3Fe_4(VO_4)_6$ and β-$Cu_3Fe_4(VO_4)_6$ structures, respectively. While these structures are reported here, the main goal of this paper is to communicate our understanding of the site-specific crystal chemistry which governs the formation of various structures and stoichiometries.

Experimental Section

Synthesis. Prior to crystal growth, a mixture of 1.345 g of $Co_3O_{4.24}$ (certified reagent, Fisher), 1.756 g of Fe_2O_3 (99+%, Aldrich), and 3.000 g of V_2O_5 (99.6%, Aldrich) powders were ground in an agate mortar and calcined in an alumina boat at 700 °C for 15 h in air. The oxygen content of cobalt oxide was determined by thermogravimetric analysis (TGA, TA Instruments Thermal Analyst 2000) in 7% H_2/93% N_2 at 800 °C for 3 h. The starting composition corresponds to "$Co_3Fe_4(VO_4)_6$". The calcined powder was packed in a platinum crucible, heated at 180 °C h^{-1} to 1010 °C, cooled to 830 °C at 6 °C h^{-1}, and further cooled to room temperature at 120 °C h^{-1}. Many dark needle crystals were formed on the top of melt. A total weight loss of 13.5% was observed owing to the evaporation of vanadium oxide and loss of oxygen from cobalt oxide. Powder X-ray diffraction (XRD) data of the crystals revealed a pattern similar to that of $Mg_{2.5}VMoO_8$. The melting point of the powdered crystals was determined by differential thermal analysis (DTA) to be 995 °C in static air. This compound melts incongruently and becomes completely liquid above 1017 °C. The

* Corresponding author.

(1) Zubkov, V. G.; Leonidov, I. A.; Poeppelmeier, K. R.; Kozhevnikov, V. L. *J. Solid State Chem.* **1994**, *111*, 197−201.
(2) Wang, X.; Stern, C. L.; Poeppelmeier, K. R. *J. Alloys Compd.* **1996**, *243*, 51−58.
(3) Wang, X.; Heier, K. R.; Stern, C. L.; Poeppelmeier, K. R. *J. Alloys Compd.* **1997**, *255*, 190−194.
(4) Wang, X.; Heier, K. R.; Stern, C. L.; Poeppelmeier, K. R. *J. Alloys Compd.* **1998**, *267*, 79−85.
(5) Ibers, J. A.; Smith, G. W. *Acta Crystallogr.* **1964**, *17*, 190−197.
(6) Katz, L.; Kasenally, A.; Kihlborg, L. *Acta Crystallogr.* **1971**, *B27*, 2071−2077.
(7) Szillat, H.; Müller-Buschbaum, Hk. *Z. Naturforsch.* **1995**, *B50*, 247−251.
(8) Hughes, J. M.; Starkey, S. J.; Malinconico, M. L.; Malinconico, L. L. *Am. Mineral.* **1987**, *72*, 1000−1005.
(9) Lafontaine, M. A.; Grenéche, J. M.; Laligant, Y.; Férey, G. *J. Solid State Chem.* **1994**, *108*, 1−10.
(10) Harding, W. D.; Kung, H. H.; Kozhevnikov, V. L.; Poeppelmeier, K. R. *J. Catal.* **1993**, *144*, 597−610.
(11) Wang, X.; Vander Griend, D. A.; Poeppelmeier, K. R. *J. Alloys Compd.*, accepted for publication.

10.1021/ic9909274 CCC: $19.00
Published on Web 12/16/1999

Table 1. Crystallographic Data

chem formula	$Co_4Fe_{3.33}(VO_4)_6$	$Mn_3Fe_4(VO_4)_6$
fw	1110.78	1077.84
space group	*Pnma* (No. 62)	$P\bar{1}$ (No. 2)
a, Å	4.965(1)	6.703(2)
b, Å	10.211(1)	8.137(1)
c, Å	17.188(3)	9.801(2)
α, deg	90.0	105.56(1)
β, deg	90.0	105.58(2)
γ, deg	90.0	102.35(1)
V, Å^3	871.4(2)	471.9(2)
Z	2	1
ρ_{calc}, g/cm^3	4.23	3.79
T, °C	−120	−120
λ, Å	0.710 69	0.710 69
μ, mm^{-1}	9.55	7.84
R^a	0.033	0.043
$R_w{}^b$	0.040	0.053

[a] $R = \sum||F_o| - |F_c||/\sum|F_o|$. [b] $R_w = [\sum w(|F_o| - |F_c|)^2/\sum w|F_o|^2]^{1/2}$; $w = 1/\sigma^2(F_o)$.

average atomic ratios of the metal species in the crystals were determined by energy dispersive analysis of X-ray (EDAX, Hitachi, Pioneer S-4500 SEM) to be Co:Fe:V = 4.1:3.4:6.0 indicative of the stoichiometry $Co_4Fe_{3.33}(VO_4)_6$. The atomic ratio Co:V of the investigated crystal was also determined by ICP-AES (inductively coupled plasma atomic emission spectrophotometry, Thermo Jarrell Ash, Atomscan 25) to be 4.1(1):6.

About 10 g of polycrystalline $Co_4Fe_{3.33}(VO_4)_6$ was prepared via standard solid-state reaction of $Co_3O_{4.24}$, Fe_2O_3, and V_2O_5. Stoichiometric amounts of the oxides were ground in an agate mortar and calcined at 670 °C for 30 h. The samples were reground, pressed into pellets, and heated in an alumina boat at 900 °C for 11 h and then 930 °C for 55 h. Each pellet increased about 70% in volume presumably due to the evolution of oxygen from cobalt oxide during the heating procedure.

$Mn_3Fe_4(VO_4)_6$ crystals were grown by melting a mixture of 1.758 g of Mn_2O_3 (99.9%, ERAC), 2.370 g of Fe_2O_3, and 4.050 g of V_2O_5 which corresponds to the composition "$Mn_3Fe_4(VO_4)_6$". A platinum crucible was used to preheat the mixture at 670 °C for 18 h in air to allow the three oxides to react with each other and reduce the evaporation of vanadium oxide. The mixture was then heated at 1050 °C for 2 h, cooled to 800 °C at 6 °C h^{-1}, and finally cooled to room temperature at 120 °C h^{-1} all in flowing argon. This atmosphere promotes the formation of $Mn_3Fe_4(VO_4)_6$ by reducing Mn^{3+} to Mn^{2+}. A total weight loss of 2.4% was observed owing to the evaporation of vanadium oxide and loss of oxygen from Mn_2O_3. Dark crystals were readily separated from the rest of melt, and the atomic ratios were determined by EDAX to be Mn:Fe:V = 3.1:4.3:6.0, indicative of $Mn_3Fe_4(VO_4)_6$.

Polycrystalline $Mn_3Fe_4(VO_4)_6$ was prepared via solid-state reaction of Mn_2O_3, Fe_2O_3, and V_2O_5 at 870 °C for 48 h in flowing nitrogen. The weight loss during the formation of $Mn_3Fe_4(VO_4)_6$ was monitored by TGA at 800 °C for 5 h under nitrogen. The total weight loss of 2.3% is consistent with the calculated value 2.2% for the reduction of Mn^{3+} to Mn^{2+}. The melting point of $Mn_3Fe_4(VO_4)_6$ was determined by DTA to be 918 °C in air.

Crystallographic Determination. A dark $Co_4Fe_{3.33}(VO_4)_6$ needle ($0.70 \times 0.08 \times 0.02$ mm^3) and a dark $Mn_3Fe_4(VO_4)_6$ prism ($0.38 \times 0.35 \times 0.20$ mm^3) were mounted on glass fibers for study by single-crystal X-ray diffraction. All measurements were made on an Enraf-Nonius CAD4 diffractometer with graphite-monochromated Mo Kα radiation. Details of the structure determinations and refinements are listed in Table 1. Analytical absorption corrections were applied,[12] which resulted in transmission factor ranges of 0.48−0.83 for $Co_4Fe_{3.33}(VO_4)_6$ and 0.09−0.26 for $Mn_3Fe_4(VO_4)_6$.

The observed systematic absences ($0kl$, $k + l = 2n + 1$; $hk0$, $h = 2n + 1$) for $Co_4Fe_{3.33}(VO_4)_6$ are consistent with the space groups *Pnma* and $Pn2_1a$. The structure was solved by direct methods[13] and expanded using Fourier techniques.[14] It refined satisfactorily in the centrosymmetric space group *Pnma*. All atoms were refined anisotropically except for the disordered atoms Co(1) and Fe(1). The formula was confirmed by chemical analysis and population refinements. Similarly, the structure of $Mn_3Fe_4(VO_4)_6$ was solved in the space group $P\bar{1}$. All atoms were refined anisotropically. Population refinements indicate that disordering between Fe^{3+} and Mn^{2+} does not take place. All calculations were performed using the TEXSAN crystallographic software package of Molecular Structure Corp.[15] Atomic positions, thermal displacement parameters, and occupancies are presented in Tables 2 and 3.

Table 2. Atomic Parameters for the $Co_4Fe_{3.33}(VO_4)_6$ Structure

atom	pos	*x*	*y*	*z*	occ	B_{eq}/B_{iso} (Å^2)
Fe(1)	8*d*	−0.2484(2)	0.5767(1)	0.52770(4)	0.83	0.32(2)[b]
Co(1)	8*d*	−0.2484(2)	0.5767(1)	0.52770(4)	0.17	0.32(2)[b]
Co(2)	4*c*	−0.096(1)	0.75	0.2493(1)	0.662(4)	2.0(1)
Co(3)	4*c*	−0.7545(2)	0.25	0.3031(1)	1.0	0.46(2)
V(1)	4*c*	0.2208(3)	0.75	0.4433(1)	1.0	0.39(3)
V(2)	8*d*	−0.2788(2)	0.4715(1)	0.3432(1)	1.0	0.37(2)
O(1)	8*d*	−0.085(1)	0.3742(4)	0.2865(2)	1.0	0.7(1)
O(2)	8*d*	−0.348(1)	0.6145(4)	0.2959(2)	1.0	0.7(1)
O(3)	8*d*	−0.087(1)	0.5051(4)	0.4253(2)	1.0	0.5(1)
O(4)	8*d*	−0.569(1)	0.3861(4)	0.3725(2)	1.0	0.5(1)
O(5)	4*c*	−0.066(1)	0.75	0.5058(4)	1.0	0.6(1)
O(6)	8*d*	0.417(1)	0.8845(4)	0.4648(3)	1.0	0.7(1)
O(7)	4*c*	0.148(1)	0.75	0.3478(1)	1.0	0.7(1)

[a] $B_{eq} = {}^8/_3\pi^2(U_{11}(aa^*)^2 + U_{22}(bb^*)^2 + U_{33}(cc^*)^2 + 2U_{12}aa^*bb^* \cos\gamma + 2U_{13}aa^*cc^* \cos\beta + 2U_{23}bb^*cc^* \cos\alpha)$. [b] Isotropic refinement.

Table 3. Atomic Parameters and Bond Valences for the $Mn_3Fe_4(VO_4)_6$ Structure

atom	pos	*x*	*y*	*z*	B_{eq} (Å^2)[a]	BV
Mn(1)	1*d*	−0.5	1.0	0.0	2.05(3)	1.95
Mn(2)	2*i*	−0.2171(1)	0.7987(1)	0.2946(1)	0.51(1)	2.40
Fe(1)	2*i*	0.1206(1)	0.5469(1)	−0.1076(1)	0.38(1)	2.93
Fe(2)	2*i*	−0.5450(1)	0.2924(1)	−0.5160(1)	0.39(1)	3.00
V(1)	2*i*	−0.3961(1)	0.5903(1)	−0.1673(1)	0.28(1)	5.03
V(2)	2*i*	0.2779(1)	0.8437(1)	0.2292(1)	0.33(1)	5.01
V(3)	2*i*	0.0988(1)	0.7685(1)	0.6275(1)	0.42(1)	5.08
O(1)	2*i*	−0.6316(5)	0.4669(4)	−0.1525(4)	0.6(1)	2.13
O(2)	2*i*	0.487(1)	0.7853(5)	0.3361(4)	0.7(1)	2.10
O(3)	2*i*	−0.149(1)	0.7580(5)	0.4978(4)	1.0(1)	2.02
O(4)	2*i*	0.030(1)	0.7317(4)	0.2312(4)	0.7(1)	2.11
O(5)	2*i*	−0.680(1)	0.0603(4)	−0.6898(4)	0.8(1)	2.02
O(6)	2*i*	−0.369(1)	0.8006(4)	−0.0834(4)	0.7(1)	2.48
O(7)	2*i*	−0.233(1)	0.9812(5)	0.7608(5)	1.6(1)	2.05
O(8)	2*i*	−0.168(1)	0.5345(4)	−0.0779(4)	0.5(1)	2.05
O(9)	2*i*	−0.427(1)	0.5528(4)	−0.3569(4)	0.5(1)	2.09
O(10)	2*i*	0.2838(5)	0.7998(4)	0.0448(4)	0.5(1)	2.33
O(11)	2*i*	−0.262(1)	0.2852(5)	−0.5315(4)	0.8(1)	2.00
O(12)	2*i*	0.060(1)	0.6297(5)	−0.2748(4)	1.0(1)	2.03

[a] See Table 2.

X-ray Measurements. XRD data for polycrystalline $Co_4Fe_{3.33}(VO_4)_6$ and $Mn_3Fe_4(VO_4)_6$ were collected on a Rigaku X-ray diffractometer with Cu Kα radiation and nickel filter in the 2θ range of 10−60° (step scan: 0.05°/4 s, Si as internal standard) at 25 °C. The observed and calculated d_{hkl} values and relative intensities I/I_0 for the powder XRD patterns of $Co_4Fe_{3.33}(VO_4)_6$ and $Mn_3Fe_4(VO_4)_6$ are given in the Supporting Information. The calculated unit cell parameters agree with the values from the single-crystal refinements.

(12) de Meulenaer, J.; Tompa, H. *Acta Crystallogr*. **1965**, *19*, 1014−1018.

(13) Sheldrick, G. M. SHELX86. In *Crystallographic Computing 3*; Sheldrick, G. M., Krüger, C., Goddard, R., Eds.; Oxford University Press: London/New York, 1985; pp 175−189.

(14) Beurskens, P. T.; Admiraal, G.; Beurskens, G.; Bosman, W. P.; Garcia-Granda, S.; Gould, R. O.; Smits, G. M. M.; Smykalla, C. DIRDIF92. In *The DIRDIF program* system; Technical Report of the Crystallography Laboratory; University of Nijmegen: Nijmegen, The Netherlands, 1992.

(15) *TEXSAN*: *Crystal Structure Analysis Package*; Molecular Structure Corporation: The Woodlands, TX, 1985.

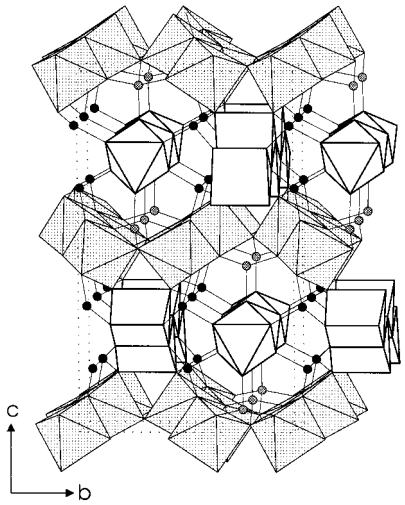

Figure 1. Structure of $Co_4Fe_{3.33}(VO_4)_6$ viewed along the *a* axis. Fully shaded circles: V(1). Partially shaded circles: V(2). Faced-shared octahedra: $Co(2)O_6$. Trigonal prisms: $Co(3)O_6$. Shaded octahedra: $Fe(1)/Co(1)O_6$. Dashed lines: unit cell.

Results and Discussion

$Co_4Fe_{3.33}(VO_4)_6$. The basic strategy for crystal growth mimics that for $Mg_{2.5}VMoO_8$.[2] Both the flux composition, "$Co_3Fe_4(VO_4)_6$", and the crystal composition, $Co_4Fe_{3.33}(VO_4)_6$, are located on the line between $Co_3V_2O_8$ and $FeVO_4$ in the $CoO-Fe_2O_3-V_2O_5$ system. Any composition along this line can be written as $Co_{3x}Fe_{6-2x}(VO_4)_6$. "$Co_3Fe_4(VO_4)_6$" and $Co_4Fe_{3.33}(VO_4)_6$ correspond to $x = 1$ and $x = 1.33$, respectively. Notice that the amount of vanadium does not change relative to the oxygen content but that the amount of low-valent cations increases. This is the opposite of the $Mg_{2.5}VMoO_8$ case in which the crystals ($Mg_{6+y}Mo_{6-2y}V_{2y}O_{24}$, $y = 1.5$) contain less low-valent cations per O^{2-} than the starting composition ($Mg_{6+y}Mo_{6-2y}V_{2y}O_{24}$, $y = 2$). In both cases the final structure is the same and the ratio of low-valent cations to high-valent cations approaches 1.23 while the oxygen content remains constant.

$Co_4Fe_{3.33}(VO_4)_6$ is a homeotype of $NaCo_{2.31}(MoO_4)_3$, $Mg_{2.5}VMoO_8$, and lyonsite, α-$Cu_3Fe_4(VO_4)_6$. The oxygen framework for this structure creates three different cation sites for low-valent cations (oxidation state I, II, or III): face-shared octahedral sites, edge/corner-shared octahedral sites, and edge-shared trigonal prismatic sites (Figure 1and Table 4). In addition, high-valent cations (V^{5+}, Mo^{6+}, V^{5+}/Mo^{6+}, or V^{5+}/W^{6+})[16] occupy two types of isolated tetrahedral sites within the framework. The details of the oxygen connectivity with the high-valent cations have been described previously for $Mg_{2.5}VMoO_8$.[2] The title compound can be written out in terms of the framework sites described above: $[Co(2)_{2/3}O_3]_2[Co(1)_{1/6}Fe(1)_{5/6}O_3]_4$ $[Co(3)O_3]_2V_6$. The face-shared octahedral site is $^2/_3$ occupied by Co which is the lowest occupation observed except for in α-$Cu_3Fe_4(VO_4)_6$.

A defining characteristic of this structure type is the high ratio of low-valent cations to high-valent cations. All synthesized examples to date exhibit a ratio between 1.22 and 1.27 which corresponds to an occupancy on the face-shared site between 0.66 and 0.81, respectively, when the other sites are fully occupied. The structure of $Co_4Fe_{3.33}(VO_4)_6$ achieves a 1.22 ratio of Co/Fe to V by incorporating extra Co^{2+} and less Fe^{3+} relative to the reactant stoichiometry (ratio = 1.17). This is the only known example of this type of behavior in these iron/vanadium systems and is facilitated by the versatility of cobalt to occupy all three framework sites. If 66% occupancy is the lower limit for stabilizing this structure when synthesized under laboratory conditions, then $Co_4Fe_{3.33}(VO_4)_6$ represents the stoichiometry nearest to the reaction stoichiometry which facilitates said structure. The occupancy of the face-shared site, and therefore the ratio of low-valent to high-valent cations, could, in principle, be increased by changing the ratio of cobalt to iron ($[Co_{2/3+x}O_3]_2[Co_{1/6+x}Fe_{5/6-x}O_3]_4$ $[CoO_3]_2V_6$). This might well be accomplished by choosing a more appropriate reactant stoichiometry. The fact that the face-shared site in $Mg_{2.5+x}V_{1+2x}Mo_{1-2x}O_8$ is limited to 81% occupancy suggests that there is also an upper bound for this structure type. The 75% Co^{2+} occupancy in $NaCo_{2.31}(MoO_4)_3$ further suggests that the upper bound has not been achieved in the present case.

(16) Wang, X.; Pless, J.; Poeppelmeier, K. R. Manuscript in preparation.

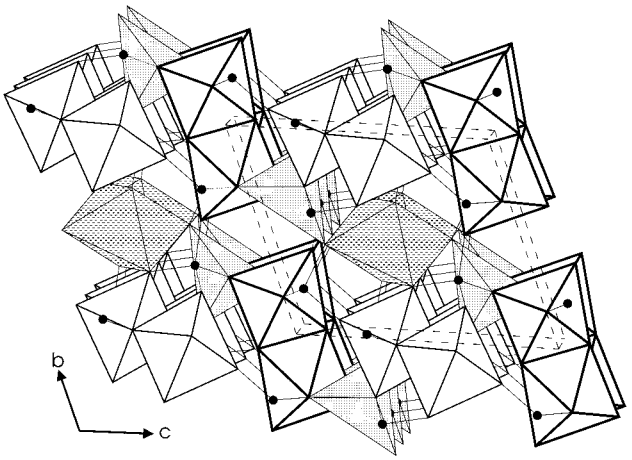

Figure 2. Structure of $Mn_3Fe_4(VO_4)_6$ viewed along the *a* axis. Shaded octahedra: $Mn(1)O_6$. Shaded trigonal bipyramids: $Mn(2)O_5$. Thin-lined Octahedra: $Fe(1)O_6$. Thick-lined octahedra: $Fe(2)O_6$. Solid circles: V.

Table 4. Selected Distances and Bond Angles for $Co_4Fe_{3.33}(VO_4)_6$

Distances (Å)			
Co(1)−O(3)	2.068(4)	Co(3)−O(1)	2.166(4) × 2
Co(1)−O(3)	2.030(4)	Co(3)−O(4)	2.049(4) × 2
Co(1)−O(4)	1.977(4)	V(1)−O(5)	1.785(6)
Co(1)−O(5)	2.023(3)	V(1)−O(6)	1.723(4) × 2
Co(1)−O(6)	2.023(4)	V(1)−O(7)	1.680(6)
Co(1)−O(6)	2.137(4)	V(2)−O(1)	1.693(4)
Co(2)−O(2)	2.010(5) × 2	V(2)−O(2)	1.706(4)
Co(2)−O(2)	2.028(5) × 2	V(2)−O(3)	1.737(4)
Co(2)−O(7)	2.083(7)	V(2)−O(4)	1.759(4)
Co(2)−O(7)	2.097(7)	Co(2)−Co(2)	2.4826(5)
Co(3)−O(1)	2.092(4) × 2		

Bond angles (deg)			
O(1)−Co(3)−O(1)	74.6(2)	O(6)−V(1)−O(6)	105.8(3)
O(1)−Co(3)−O(1)	81.6(1) × 2	O(6)−V(1)−O(7)	109.3(2) × 2
O(1)−Co(3)−O(1)	71.7(2)	O(1)−V(2)−O(2)	110.0(2)
O(1)−Co(3)−O(4)	80.9(2) × 2	O(1)−V(2)−O(3)	105.7(2)
O(1)−Co(3)−O(4)	91.1(2) × 2	O(1)−V(2)−O(4)	109.9(2)
O(4)−Co(3)−O(4)	85.4(2)	O(2)−V(2)−O(3)	109.2(2)
O(5)−V(1)−O(6)	108.7(2) × 2	O(2)−V(2)−O(4)	113.3(2)
O(5)−V(1)−O(7)	114.7(3)	O(3)−V(2)−O(4)	108.4(2)

$Mn_3Fe_4(VO_4)_6$. $Mn_3Fe_4(VO_4)_6$ is a homeotype of β-$Cu_3Fe_4(VO_4)_6$[9] since MnO_6 octahedra in the former replace CuO_4 square planes in the latter. The structure is built up from FeO_6 octahedra, MnO_6 octahedra, MnO_5 trigonal bipyramids, and isolated VO_4 tetrahedra (Figure 2 and Table 5). The linkage between the octahedra and bipyramids is shown in Figure 3. MnO_5 bipyramids alternate with Fe_2O_{10} octahedral dimers to form edge-sharing chains. The MnO_6 octahedra are located between the chains and share corners with both the MnO_5 and Fe_2O_{10} units.

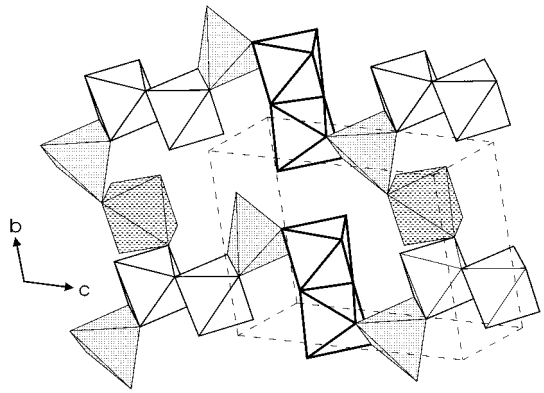

Figure 3. Connections of MnO_6 and MnO_5 polyhedra with Fe_2O_{10} octahedral dimers in $Mn_3Fe_4(VO_4)_6$.

Table 5. Selected Distances and Bond Angles for $Mn_3Fe_4(VO_4)_6$

Distances (Å)			
Fe(1)−O(1)	2.019(4)	Mn(2)−O(3)	2.053(4)
Fe(1)−O(4)	2.125(3)	Mn(2)−O(4)	2.043(4)
Fe(1)−O(8)	2.015(4)	Mn(2)−O(7)	2.022(4)
Fe(1)−O(8)	2.066(3)	V(1)−O(1)	1.744(3)
Fe(1)−O(10)	2.043(3)	V(1)−O(6)	1.634(3)
Fe(1)−O(12)	1.913(4)	V(1)−O(8)	1.764(4)
Fe(2)−O(2)	1.998(3)	V(1)−O(9)	1.747(3)
Fe(2)−O(3)	2.068(4)	V(2)−O(2)	1.749(4)
Fe(2)−O(5)	2.000(3)	V(2)−O(4)	1.726(4)
Fe(2)−O(9)	1.998(3)	V(2)−O(5)	1.654(3)
Fe(2)−O(9)	2.097(3)	V(2)−O(10)	1.759(3)
Fe(2)−O(11)	1.954(4)	V(3)−O(3)	1.770(4)
Mn(1)−O(6)	2.086(3) × 2	V(3)−O(7)	1.732(4)
Mn(1)−O(7)	2.481(5) × 2	V(3)−O(11)	1.677(4)
Mn(1)−O(10)	2.159(3) × 2	V(3)−O(12)	1.687(4)
Mn(2)−O(1)	2.080(3)	Fe(1)−Fe(1)	3.132(1)
Mn(2)−O(2)	2.113(4)	Fe(2)−Fe(2)	3.215(1)

Bond angles (deg)			
O(6)−Mn(1)−O(6)	180.0	O(1)−Mn(2)−O(4)	77.8(1)
O(6)−Mn(1)−O(7)	99.9(1) × 2	O(2)−Mn(2)−O(3)	77.8(1)
O(6)−Mn(1)−O(7)	80.1(1) × 2	O(2)−Mn(2)−O(7)	89.1(2)
O(6)−Mn(1)−O(10)	87.1(1) × 2	O(3)−Mn(2)−O(4)	99.7(1)
O(6)−Mn(1)−O(10)	92.9(1) × 2	O(4)−Mn(2)−O(7)	104.3(2)
O(7)−Mn(1)−O(7)	180.0	O(1)−Mn(2)−O(3)	98.6(1)
O(7)−Mn(1)−O(10)	96.1(1) × 2	O(1)−Mn(2)−O(7)	126.5(2)
O(7)−Mn(1)−O(10)	83.9(1) × 2	O(3)−Mn(2)−O(7)	132.2(2)
O(10)−Mn(1)−O(10)	180.0	O(2)−Mn(2)−O(4)	163.1(1)
O(1)−Mn(2)−O(2)	86.0(1)		

The Fe_2O_{10} octahedral dimers are surrounded by either 8 (Figure 4a) or 10 (Figure 4b) isolated VO_4 tetrahedra. The double corner connection of $Fe(1)_2O_{10}$ to $V(2)O_4$ (Figure 4a) is rare because usually the distance between two vertexes of a VO_4 tetrahedron is not long enough to span the two apices of an Fe_2O_{10} edge-shared octahedra. The Fe(1)−Fe(1) distance (3.132(1) Å) is significantly shorter than even the Fe(2)−Fe(2) (3.212(1) Å), as well as the corresponding distances in isolated Fe_2O_{10} dimers found in $FeVMoO_7$, $Fe_2V_3MoO_{13.5}$, and $Fe_2V_4O_{13}$.[17,18] Within each MnO_6 unit two bonds are substantially elongated, indicating a strong octahedral distortion. Such a distortion could be a Jahn−Teller effect if the Mn is +3. Structural refinement, bond valence calculations (see Table 3),[19] and TGA weight loss all concur however that not only is the iron Fe^{3+} and the vanadium V^{5+} but that the manganese is Mn^{2+}. Therefore, the distortion must be attributed to interpolyhedral connections, such as observed in $Mn_3O(SeO_3)_3$.[20] It is likely that the position of the crystallographically independent oxygen (O(7)) is determined by other polyhedra. This explanation is supported by the presence of the CuO_4 square planes in β-$Cu_3Fe_4(VO_4)_6$. O(7) also has relatively large temperature factor (Table 3), and the thermal ellipsoid elongates in the direction of the Mn(1)−O(7) bonds. Since Mn^{2+} is a d^5 cation, the enlarged temperature factor in the octahedra is likely due to these same interpolyhedral stresses and negligible ligand field stabilization.

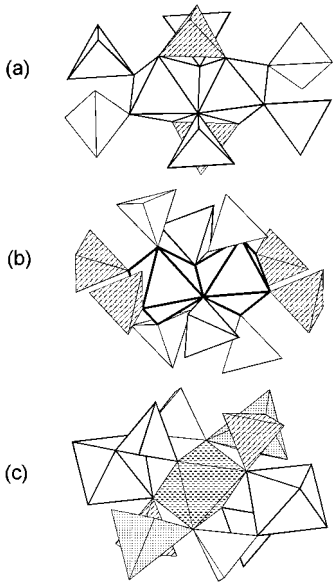

Figure 4. (a) Eight VO_4 tetrahedra surrounding $Fe(1)_2O_{10}$ octahedral dimer. Spanning tetrahedra ($V(2)O_4$) are shaded. (b) Ten VO_4 tetrahedra surrounding the $Fe(2)_2O_{10}$ octahedral dimer. $V(2)O_4$ tetrahedra are shaded. (c) Connections of MnO_6 with adjacent polyhedra. Symbols are consistent with those in Figure 2.

MnO_5 square pyramids are quite common, being found in brownmillerite-related compounds such as $Ca_2Mn_2O_5$,[21,22] $Ca_2MnO_{3.5}$,[23] and $Ca_3Fe_{1.65}Mn_{1.35}O_{8.02}$,[24] but $Mn^{2+}O_5$ trigonal bipyramids are very unusual. To our knowledge, the only MnO_5 trigonal bipyramids reported exist in such oxides as $Lu_3MnFe_3O_{10}$[25] and $Lu_4MnFe_4O_{13}$,[26] where the manganese is disordered with the iron. The bond angles in the title compound do deviate slightly from ideal trigonal bipyramidal coordination toward square pyramidal geometry.

The ratio of low-valent cations to high-valent cations in the manganese phase is 1.17 and does not differ from the reactant stoichiometry. This indicates either the unavailability of the α-$Cu_3Fe_4(VO_4)_6$ structure type or the particular stability of the β-$Cu_3Fe_4(VO_4)_6$ structure type for the manganese case. The former possibility is debased by the fact that Mn^{2+} is known to occupy the face-shared octahedral and trigonal prismatic sites of the β-$Cu_3Fe_4(VO_4)_6$ structure type in $Mn_{2.47}V_{0.94}Mo_{1.06}O_8$.

General Comments. The molar density of $Co_4Fe_{3.33}(VO_4)_6$ is greater than that of $Mn_3Fe_4(VO_4)_6$. This is a result of the

(17) Wang, X.; Heier, K. R.; Stern, C. L.; Poeppelmeier, K. R. *Inorg. Chem.* **1998**, *37*, 3252−3256.
(18) Wang, X.; Heier, K. R.; Stern, C. L.; Poeppelmeier, K. R. *Inorg. Chem.* **1998**, *37*, 6921−6927.
(19) Brown, I. D.; Altermatt, D. *Acta Crystallogr.* **1985**, *B41*, 244−247.
(20) Wildner, M. *J. Solid State Chem.* **1994**, *113*, 252−256.
(21) Poeppelmeier, K. R.; Leonowicz, M. E.; Longo, J. M. *J. Solid State Chem.* **1982**, *44*, 89−98.
(22) Poeppelmeier, K. R.; Leonowicz, M. E.; Scanlon, J. C.; Longo, J. M.; Yelon, W. B. *J. Solid State Chem.* **1982**, *45*, 71−79.
(23) Leonowicz, M. E.; Poeppelmeier, K. R.; Longo, J. M. *J. Solid State Chem.* **1985**, *59*, 71−80.
(24) Hervieu, M.; Nguyen, N.; Caignaert, V.; Raveau, B. *Phys. Status Solidi* **1984**, *A83*, 473−483.
(25) Malaman, B.; Aqachmar, E. H.; Gerardin, R.; Evrard, O. *Mater. Res. Bull.* **1991**, *26*, 937−943.
(26) Malaman, B.; Aqachmar, E. H.; Gerardin, R.; Evrard, O. *Mater. Res. Bull.* **1992**, *27*, 855−865.

higher coordination of the anions and cations. α-$Cu_3Fe_4(VO_4)_6$ ($d = 4.21$ g/cm^3) is also more closely packed than β-$Cu_3Fe_4(VO_4)_6$ ($d = 3.97$ g/cm^3) and is regarded as the high-pressure form.[9] As previously noted, it is likely that the α-$Cu_3Fe_4(VO_4)_6$ structure type is available to the manganese analogue and so should be stable under pressure. It is also possible that stabilization could be achieved by simply choosing a flux stoichiometry with more low-valent cations. As reported in this paper, the more dense cobalt analogue forms directly at ambient pressure from an off-stoichiometric starting mix. Making the less dense cobalt analogue is likely impossible unless it can be synthesized by choosing a reactant flux with even less low-valent cation, i.e. even farther from the necessary composition for the more dense phase.

The four $MO-Fe_2O_3-V_2O_5$ (M = Mg, Zn, Co, Mn) systems yielded four new ternary vanadates with three different structures,[11] but it is worthwhile to note which compounds did not form. Since growing crystals from mixed oxide fluxes generally renders thermodynamic products, it can be concluded that many of the possible polymorphic compounds within these systems are relatively unstable despite the fact that they are quite similar. The cobalt system is the only example of a structure that incorporated additional low-valent cations into an optimally dense structure. The manganese system maintained the reactant stoichiometry, while the zinc and magnesium systems expunged low-valent cations to form crystals with ratios of low-valent to high-valent cations equal to one. It can be inferred, consequently, that the two $Cu_3Fe_4(VO_4)_6$ structure types are destabilized by zinc and magnesium. The stabilities of site-specific cation occupation are the link between structure and composition. The more dense structures create less common coordination environments such as face-shared octahedra, trigonal prisms, and trigonal bipyramids and, therefore, require cations to occupy these sites at least partially. The formation of the high-density structure in general must be a complex function of composition. The fact that compounds with compositions such as "$Mg_3Fe_4(VO_4)_6$", "$Zn_4Fe_{3.33}(VO_4)_6$", "$FeCo_2V_3O_{11}$", and "$FeMn_2V_3O_{11}$" were not detected illustrates the intricacies and suggests the possibilities of the solid-state chemistry involved.

Conclusions

Crystals of $Co_4Fe_{3.33}(VO_4)_6$ and $Mn_3Fe_4(VO_4)_6$ were successfully grown from mixed metal oxide melts. Single-crystal X-ray diffraction studies revealed the details of the two structures, which have been discussed and compared with two polymorphs of $Cu_3Fe_4(VO_4)_6$ as well as other similar structures. In addition, the rare $Mn^{2+}O_5$ trigonal bipyramidal coordination was also discussed. Detailed phase diagrams of $Co/MnO-Fe_2O_3-V_2O_5$ and catalytic properties for the title compounds are under investigation.

Acknowledgment. The authors wish to thank Dr. Larry Cirjak and acknowledge an Extramural Research Award (EMRA) from BP America, Inc., the National Science Foundation, Solid State Chemistry (Award Nos. DMR-9412971 and DMR-9727516), and the use of central facilities supported by MRSEC program of the National Science Foundation (Grant DMR-9632472) at the Materials Science Center of Northwestern University. D.A.V.G. is supported by an NSF graduate fellowship.

Supporting Information Available: Two X-ray crystallographic files, in CIF format, as well as tables of observed and calculated X-ray powder diffraction data. This material is available free of charge via the Internet at http://pubs.acs.org.

IC9909274